Magnetic-field Estimation Using Measurements from a Floating Buoy

Harish J. Palanthandalam-Madapusi, Dennis S. Bernstein, and Aaron J. Ridley

Abstract— **Magnetic-field fluctuations caused by solar storms can overload and destroy transformers, power grids and sensitive instrumentation on satellites, planes, and ships. To monitor these magnetic-field fluctuations, it is proposed to install magnetometers on floating buoys in the oceans. To obtain meaningful measurements from these magnetometers, it is important to know the orientation of the axes of the magnetometers with respect to the Earth. In this paper, we estimate the orientation of a floating buoy with respect to Earth using gyro measurements of angular velocity of the buoy. Since the angular position states are unobservable from the angular velocity measurements, we construct an additional fictitious measurement based on physical insights. In addition, to accommodate the additional fictitious measurement, we use an alternative nonlinear model for the buoy dynamics and use nonlinear filtering techniques to estimate the orientation of the buoy.**

I. INTRODUCTION

The Sun's atmosphere flows supersonically away from the Sun past the Earth and the other planets in the form of the solar wind. The Sun's magnetic field, which is commonly referred to as the interplanetary magnetic field (IMF), is embedded in the solar wind [9]. Although the solar wind typically flows at about 400 km/s, large expulsions of plasma from the Sun, called coronal mass ejections (CMEs) or solar storms, can attain speeds of over 900 km/s.

High-energy CMEs interact with the Earth's magnetic field causing geomagnetic storms, which entail ionospheric currents and aurora in both the northern and southern polar regions. Most of the time, the aurora and the ionospheric currents are weak and have minimal effect on technology. During a solar storm, however, the aurora and ionospheric currents increase, heating and expanding the upper atmosphere, which causes increased drag on satellites. In addition, large ionospheric current fluctuations can induce currents in power lines that can overwhelm and destroy transformers and electrical networks [10]. Additionally, as discussed in [11], solar storms can adversely affect animals, humans, and aircraft. It is therefore important to monitor magnetic-field fluctuations caused by solar storms, to be able to predict when and where large ionospheric current fluctuations are likely to occur.

H. J. Palanthandalam-Madapusi is with the Department of Mechanical and Aerospace Engineering, 149 Link Hall, Syracuse University, Syracuse, NY 13244, hjpalant@syr.edu.
A. Girard and D. S. Bernstein are with the Department of Aerospace Engineering, The University of Michigan, Ann Arbor, MI 48109, {dsbaero,ridley}@umich.edu.

The magnetic perturbations caused by the interaction of the solar wind and the magnetosphere are measured on the Earth by ground-based magnetometer stations. Numerous ground-based magnetometer stations are spread over North America and Canada, Northern Europe, Russia, and Greenland. In addition, there are ground-based magnetometer stations, although fewer in number, in the southern hemisphere. These large number of ground-based magnetometer stations provide a good picture of the magnetic fluctuations on the surface of land masses.

However, there are no magnetometers in the oceans and the seas and magnetic-fluctuations in the oceans are not measured. Since infrastructure that may be affected by solar storms include undersea cables and instrumentation on ships and submarines, it is important to place magnetometers in several locations in the oceans. Currently, tt is being proposed that magnetometers be installed on floating buoys. In contrast to ground-based magnetometers, buoys are constantly moving due to wind and waves. Therefore to obtain meaningful measurements from the magnetometers, it is important to know the orientation of the axes of the magnetometers with respect to the Earth.

The goal of this paper is to estimate the orientation of a floating buoy with respect to Earth using gyro measurements of angular velocity of the buoy. We start with a second-order linear model for the buoy dynamics driven by random forces. Since the angular position states are unobservable from the angular velocity measurements, we construct an additional fictitious measurement based on physical insights. In addition, to accommodate the additional fictitious measurement, we construct an alternative nonlinear model for the buoy dynamics and use nonlinear filtering techniques to estimate the orientation of the buoy.

II. PROBLEM FORMULATION

For simplicity, we consider the yawing (spinning) motion of the buoy alone, that is, we assume that the buoy does not roll or pitch. Let ϕ be the yaw angle of the buoy. Then defining the states to be $x \stackrel{\triangle}{=} \begin{bmatrix} \phi & \dot{\phi} \end{bmatrix}^{\mathrm{T}}$, the equations of motion of the buoy in the state space form are

$$\dot{x} = \begin{bmatrix} 0 & 1 \\ 0 & -c \end{bmatrix} x + \begin{bmatrix} 0 \\ 1 \end{bmatrix} w, \qquad (2.1)$$

where c represents the damping coefficient due to water drag, and w represents the effect of random forces on the buoy due

to wind and waves. We assume that a rate gyro is mounted on the buoy, thus the output equation is

$$y = \begin{bmatrix} 0 & 1 \end{bmatrix} x + v, \qquad (2.2)$$

where v is the measurement noise. Thus,

$$A = \begin{bmatrix} 0 & 1 \\ 0 & -c \end{bmatrix}, \quad B = \begin{bmatrix} 0 \\ 0 \end{bmatrix} \qquad (2.3)$$

$$C = \begin{bmatrix} 0 & 1 \end{bmatrix}, \quad D = 0, \qquad (2.4)$$

and $Q \triangleq \mathbb{E}\left[\begin{bmatrix} 0 \\ w \end{bmatrix} \begin{bmatrix} 0 & w \end{bmatrix}\right] = \begin{bmatrix} 0 & 0 \\ 0 & \sigma_w^2 \end{bmatrix}$, where $\mathbb{E}$ denotes the expected value and $\sigma_w^2 \triangleq \mathbb{E}\left[w^2\right]$.

Next, let B_N and B_E denote the north-south and east-west component of the Earth's magnetic field, respectively. Let $B_T \triangleq \sqrt{B_N^2 + B_E^2}$ be the total magnetic field of the Earth and $\theta \triangleq \tan^{-1}\left(\frac{B_E}{B_N}\right)$ be the clockwise angle from the total magnetic field to the north-south direction. Next, let B_x and B_y be the components of the magnetic field measured by the magnetometer fixed on the buoy. Since ϕ is the yaw angle of the buoy, it follows that

$$B_x = B_T \cos(\phi - \theta), \qquad (2.5)$$

$$B_y = -B_T \sin(\phi - \theta). \qquad (2.6)$$

The relationship between the various components of the magnetic field are shown in Figure 1.

Throughout this paper, for simulations, we use the value $c = 0.2$ for the damping coefficient in (2.1). The disturbances w and v are chosen to be a gaussian white noise signals. The north-south component of the magnetic field B_N is chosen to be a random white signal with mean $20,000$nT, while the east-west component of the magnetic field B_E is chosen to be a random white signal with mean 0nT. These mean values are typical.

The problem can then be stated as

Problem 1. Using the magnetometer measurements B_x and B_y along with the gyro measurements of $\dot{\phi}$, estimate the components of the Earth's magnetic field B_N and B_E in the Earth-fixed coordinate frame.

From Figure 1, it follows that

$$B_N = B_x \cos(\phi) - B_y \sin(\phi), \qquad (2.7)$$

$$B_E = B_x \sin(\phi) + B_y \cos(\phi). \qquad (2.8)$$

Since, B_x and B_y are measured, Problem 1 is equivalent to the following problem.

Problem 2. Using the magnetometer measurements B_x and B_y along with the gyro measurements of $\dot{\phi}$, estimate the yaw angle ϕ of the buoy.
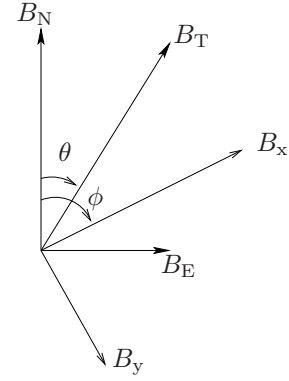

Fig. 1. Schematic of relationship between components of magnetic field in an Earth-fixed frame and body-fixed frame.

Since ϕ is an unmeasured state of the linear system (2.1), (2.2), we consider state estimation for linear systems. For ease of application of estimation techniques, we use a discrete-time version of the state-space equations (2.1), (2.2). We briefly review the Kalman filter.

A. Kalman Filter

For the linear stochastic discrete-time dynamic system

$$x_k = A_{k-1}x_{k-1} + B_{k-1}u_{k-1} + G_{k-1}w_{k-1}, \quad (2.9)$$

$$y_k = C_k x_k + v_k, \qquad (2.10)$$

where $A_{k-1} \in \mathbb{R}^{n \times n}$, $B_{k-1} \in \mathbb{R}^{n \times p}$, $G_{k-1} \in \mathbb{R}^{n \times q}$, and $C_k \in \mathbb{R}^{m \times n}$ are known matrices, the state-estimation problem can be described as follows. Assume that, for all $k \geq 1$, the known data are the measurements $y_k \in \mathbb{R}^m$, the inputs $u_{k-1} \in \mathbb{R}^p$, and the statistical properties of x_0, w_{k-1} and v_k. The initial state vector $x_0 \in \mathbb{R}^n$ is assumed to be Gaussian with mean $\hat{x}_0$ and error-covariance $P_0^{xx} \triangleq \mathbb{E}\left[(x_0 - \hat{x}_0)(x_0 - \hat{x}_0)^{\mathrm{T}}\right]$. The process noise $w_{k-1} \in \mathbb{R}^q$, which represents unknown input disturbances, and the measurement noise $v_k \in \mathbb{R}^m$, concerning inaccuracies in the measurements, are assumed white, Gaussian, zero mean, and mutually independent with known covariance matrices Q_{k-1} and R_k, respectively. Next, define the cost function

$$J(x_k) \triangleq \rho(x_k | (y_1, \ldots, y_k)), \qquad (2.11)$$

which is the conditional probability density function of the state vector $x_k \in \mathbb{R}^n$ given the past and present measured data $y_1, \ldots, y_k$. Under the stated assumptions, the maximization of (2.11) is the state estimation problem, while the maximizer $\hat{x}_k$ of J is the optimal state estimate.

The optimal state estimate $\hat{x}_k$ is given by the Kalman filter

[6], whose *forecast* step is given by

$$\hat{x}_{k|k-1} = A_{k-1}\hat{x}_{k-1} + B_{k-1}u_{k-1}, \tag{2.12}$$

$$P_{k|k-1}^{xx} = A_{k-1}P_{k-1}^{xx}A_{k-1}^{\mathrm{T}} + G_{k-1}Q_{k-1}G_{k-1}^{\mathrm{T}}, \tag{2.13}$$

$$\hat{y}_{k|k-1} = C_k\hat{x}_{k|k-1}, \tag{2.14}$$

$$P_{k|k-1}^{yy} = C_kP_{k|k-1}^{xx}C_k^{\mathrm{T}} + R_k, \tag{2.15}$$

$$P_{k|k-1}^{xy} = P_{k|k-1}^{xx}C_k^{\mathrm{T}}, \tag{2.16}$$

where $P_{k|k-1}^{xx} \triangleq \mathrm{E}\left[(x_k - \hat{x}_{k|k-1})(x_k - \hat{x}_{k|k-1})^{\mathrm{T}}\right]$, $P_{k|k-1}^{yy} \triangleq \mathrm{E}\left[(y_k - \hat{y}_{k|k-1})(y_k - \hat{y}_{k|k-1})^{\mathrm{T}}\right]$, and $P_{k|k-1}^{xy} \triangleq \mathrm{E}\left[(x_k - \hat{x}_{k|k-1})(y_k - \hat{y}_{k|k-1})^{\mathrm{T}}\right]$, and whose *data-assimilation* step is given by

$$K_k = P_{k|k-1}^{xy}(P_{k|k-1}^{yy})^{-1}, \tag{2.17}$$

$$\hat{x}_k = \hat{x}_{k|k-1} + K_k(y_k - \hat{y}_{k|k-1}), \tag{2.18}$$

$$P_k^{xx} = P_{k|k-1}^{xx} - K_kP_{k|k-1}^{yy}K_k^{\mathrm{T}}, \tag{2.19}$$

where $P_k^{xx} \triangleq \mathrm{E}\left[(x_k - \hat{x}_k)(x_k - \hat{x}_k)^{\mathrm{T}}\right]$ is the error-covariance matrix and K_k is the Kalman gain matrix. The notation $\hat{z}_{k|k-1}$ indicates an estimate of z_k at time k based on information available up to and including time $k-1$. Likewise, $\hat{z}_k$ indicates an estimate of z at time k using information available up to and including time k. Model information is used during the forecast step, while measurement data are injected into the estimates during the data-assimilation step, specifically, (2.18).

III. YAW ANGLE ESTIMATION USING GYRO MEASUREMENTS

Since (A, C) in (2.3), (2.4) is unobservable, the Kalman filter estimates $\hat{x}_k$ are not guaranteed to converge to x_k and may drift. As seen in Figure 2, due to the unobservability of the system, there is drift in the estimates.

To resolve the problem of observability, we use insights from physics to construct an additional fictitious measurement. However, as described in the following section, to accommodate this additional measurement, we modify the model equations.

IV. PHYSICS-BASED FICTITIOUS MEASUREMENT

From the knowledge of physics we know that over long periods of time, the median of the total magnetic field B_{T} points north. That is, over long periods of time, the median of θ is 0. We make the assumption that the mean of θ is also zero over a long period of time.
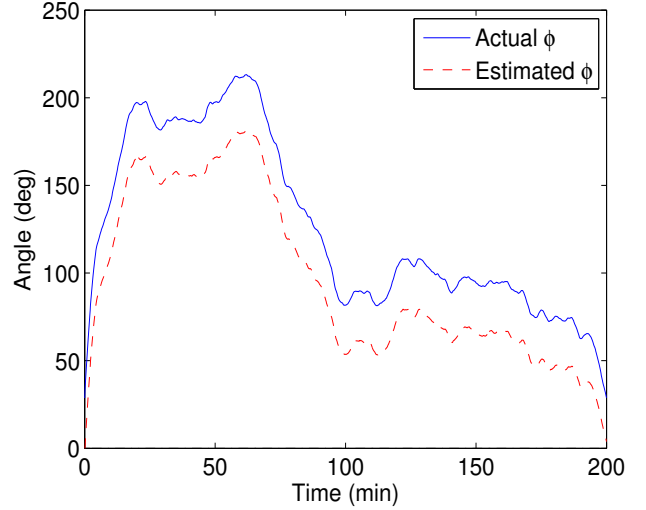

Fig. 2. Actual yaw angle and the estimate of the yaw angle using a linear Kalman filter with rate gyro measurements. Since the yaw angle is unobservable from the rate gyro measurements, the estimates do not converge to the actual angles.

First, we note that

$$\tan^{-1}\left(\frac{B_{\mathrm{y}}}{B_{\mathrm{x}}}\right) = \phi - \theta. \tag{4.1}$$

Next, let N_{w} be a sufficiently large window length. Then it follows that

$$\frac{1}{N_{\mathrm{w}}}\sum_{i=k-N_{\mathrm{w}}+1}^{k}\tan^{-1}\left(\frac{B_{\mathrm{y},i}}{B_{\mathrm{x},i}}\right)$$

$$= \frac{1}{N_{\mathrm{w}}}\sum_{i=k-N_{\mathrm{w}}+1}^{k}(\theta_i - \phi_i)$$

$$= -\frac{1}{N_{\mathrm{w}}}\sum_{i=k-N_{\mathrm{w}}+1}^{k}\phi_i. \tag{4.2}$$

The last step follows from the fact that the mean of θ over a long period of time is zero. This physics-based fictitious measurement is a function of ϕ_k from N_{w} consecutive time steps. Therefore, to use this measurement, we modify the model equations to include N_{w} time steps. Thus, by defining the states as

$$x_k = \begin{bmatrix} \phi_{k-N_{\mathrm{w}}+1} \\ \dot{\phi}_{k-N_{\mathrm{w}}+1} \\ \phi_{k-N_{\mathrm{w}}+2} \\ \dot{\phi}_{k-N_{\mathrm{w}}+2} \\ \cdots \\ \dot{\phi}_k \end{bmatrix}^{\mathrm{T}} \in \mathbb{R}^{2N_{\mathrm{w}}} \tag{4.3}$$

and writing the state-space differential equation in terms of the new state, the output equation then becomes

$$y_k = Cx_k, \tag{4.4}$$

where

$$C = \begin{bmatrix} 0 & 1 & 0 & 0 & \cdots & 0 \\ 0 & 0 & 0 & 1 & \cdots & 0 \\ \vdots & \vdots & \vdots & \vdots & \ddots & \vdots \\ 0 & 0 & 0 & 0 & \cdots & 1 \\ -\frac{1}{N_{\mathrm{w}}} & 0 & -\frac{1}{N_{\mathrm{w}}} & 0 & \cdots & 0 \end{bmatrix} \qquad (4.5)$$
$$\in \mathbb{R}^{N_{\mathrm{w}}+1 \times 2N_{\mathrm{w}}}.$$

The first N_{w} rows of C represent rate gyro measurements, while the last row represent the fictitious physics-based measurement computed from (4.2) and real measurements of $B_{\mathrm{x},k}$ and $B_{\mathrm{y},k}$.

Augmenting the measurement equations with the physics-based fictitious measurement described above makes the system equations observable. The effect of the additional physics-based fictitious measurement is aparent in Figure 3, where the estimates of the yaw angle of the buoy match the actual yaw angle.
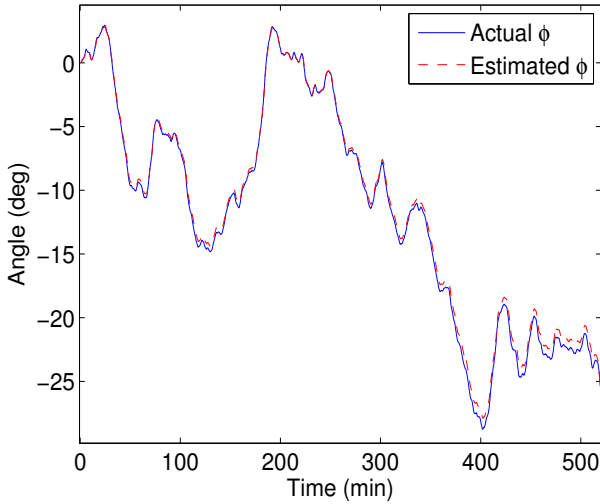

Fig. 3. Actual yaw angle of the buoy and it's estimate. For small angles, a linear Kalman filter based on the linear model equations and the rate gyro measurements along with the physics-based fictitious measurement provides an accurate estimate of the actual yaw angle.

However, note that the computed value of $\frac{1}{N_{\mathrm{w}}}\sum_{i=k-N_{\mathrm{w}}+1}^{k} \tan^{-1}\left(\frac{B_{\mathrm{y},i}}{B_{\mathrm{x},i}}\right)$ is always in the interval $(-\pi/2, \pi/2)$ radians due to the ambiguity in computing the arctangent function. On the other hand, due to the linear nature of the state equations, the angle $\phi_k \in \mathbb{R}$, and is not constrained to the interval $(-\pi/2, \pi/2)$. Due to this ambiguity, the physics-based fictitious measurement is not suitable to be used with the model equations in the current form.

To illustrate this issue, let $N_{\mathrm{w}} = 2$ and let $\phi_{k-1} = 0$ and $\phi_k = 2\pi$. Now $\tan^{-1}\left(\frac{B_{\mathrm{y},k-1}}{B_{\mathrm{x},k-1}}\right) = 0$ and $\tan^{-1}\left(\frac{B_{\mathrm{y},k}}{B_{\mathrm{x},k}}\right) = 0$. Although the physics-based fictitious measurements are consistent with the actual angles, the averages computed on the left hand side of (4.2) yields 0, while the average on the right hand side yields π. Figure 4 illustrates this issue as the estimates of the yaw angle do not match the actual angles when the actual angles are beyond the interval $(-\pi/2, \pi/2)$ radians. Note that the estimates do not differ from the actual yaw angle by a multiple of 2π radians, and thus are not accurate estimates.

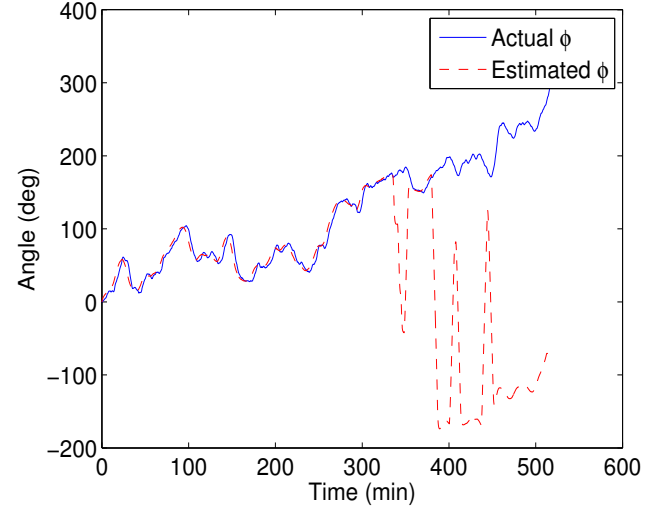To eliminate this ambiguity, we consider the following alternative representation of the model equations.

Fig. 4. Actual yaw angle of the buoy and it's estimate. For large angles, a linear Kalman filter based on the linear model equations and the rate gyro measurements along with the physics-based fictitious measurement does not provides an accurate estimate of the actual yaw angle.

V. ALTERNATIVE REPRESENTATION OF MODEL EQUATIONS

Instead of states ϕ and $\dot{\phi}$, we consider the 3 states $\sin(\phi)$, $\cos(\phi)$, and $\dot{\phi}$.

$$x_1 = \sin(\phi), \qquad (5.1)$$
$$x_2 = \cos(\phi), \qquad (5.2)$$
$$x_3 = \dot{\phi}. \qquad (5.3)$$

The differential equations in terms of these new states are then

$$\dot{x}_1 = \cos(\phi)\dot{\phi} = x_2 x_3, \qquad (5.4)$$
$$\dot{x}_2 = -\sin(\phi)\dot{\phi} = -x_1 x_3, \qquad (5.5)$$
$$\dot{x}_3 = -c\dot{\phi} + w = -cx_3 + w. \qquad (5.6)$$

The third equation is identical to the second equation in (2.1). To use the fictitious physics-based measurement, we again use a window of N_{w} time-steps.

However, in this alternative representation, the state equations are nonlinear and hence we use the unscented Kalman filter.

A. Unscented Kalman Filter

For nonlinear systems, we consider the unscented Kalman filter (UKF) [4] to provide a suboptimal solution to the state-estimation problem. Instead of analytically linearizing (5.4)-(5.6) and using (2.12)-(2.19), UKF employs the unscented transform (UT) [5], which approximates the posterior mean $\hat{y} \in \mathbb{R}^m$ and covariance $P^{yy} \in \mathbb{R}^{m \times m}$ of a random vector y obtained from the nonlinear transformation $y = h(x)$, where x is a prior random vector whose mean $\hat{x} \in \mathbb{R}^n$ and covariance $P^{xx} \in \mathbb{R}^{n \times n}$ are assumed known. UT yields the actual mean $\hat{y}$ and the actual covariance P^{yy} if $h = h_1 + h_2$, where h_1 is linear and h_2 is quadratic [5]. Otherwise, $\hat{y}_k$ is a *pseudo mean* and P^{yy} is a *pseudo covariance*.

UT is based on a set of deterministically chosen vectors known as sigma points. To capture the mean $\hat{x}^{\mathrm{a}}_{k-1}$ of the augmented prior state vector

$$x^{\mathrm{a}}_{k-1} \triangleq \begin{bmatrix} x_{k-1} \\ w_{k-1} \end{bmatrix}, \tag{5.7}$$

where $x^{\mathrm{a}}_{k-1} \in \mathbb{R}^{n_{\mathrm{a}}}$ and $n_{\mathrm{a}} \triangleq n + q$, as well as the augmented prior error covariance

$$P^{xx\mathrm{a}}_{k-1} \triangleq \begin{bmatrix} P^{xx}_{k-1|k-2} & 0_{n \times q} \\ 0_{q \times n} & Q_{k-1} \end{bmatrix}, \tag{5.8}$$

the sigma-point matrix $\mathfrak{X}_{k-1} \in \mathbb{R}^{n_{\mathrm{a}} \times (2n_{\mathrm{a}}+1)}$ is chosen as

$$\begin{cases} \mathrm{col}_0(\mathfrak{X}_{k-1}) & \triangleq \hat{x}^{\mathrm{a}}_{k-1}, \\ \mathrm{col}_i(\mathfrak{X}_{k-1}) & \triangleq \hat{x}^{\mathrm{a}}_{k-1} \\ & \quad + \sqrt{(n_{\mathrm{a}} + \lambda)}\, \mathrm{col}_i \left[\left(P^{xx\mathrm{a}}_{k-1} \right)^{1/2} \right], \\ & \quad i = 1, \dots, n_{\mathrm{a}}, \\ \mathrm{col}_{i+n_{\mathrm{a}}}(\mathfrak{X}_{k-1}) & \triangleq \hat{x}^{\mathrm{a}}_{k-1} \\ & \quad - \sqrt{(n_{\mathrm{a}} + \lambda)}\, \mathrm{col}_i \left[\left(P^{xx\mathrm{a}}_{k-1} \right)^{1/2} \right], \\ & \quad i = 1, \dots, n_{\mathrm{a}}, \end{cases}$$

with weights

$$\begin{cases} \gamma_0^{(m)} & \triangleq \dfrac{\lambda}{n_{\mathrm{a}} + \lambda}, \\ \gamma_0^{(c)} & \triangleq \dfrac{\lambda}{n_{\mathrm{a}} + \lambda} + 1 - \alpha^2 + \beta, \\ \gamma_i^{(m)} & \triangleq \gamma_i^{(c)} \triangleq \gamma_{i+n_{\mathrm{a}}}^{(m)} \triangleq \gamma_{i+n_{\mathrm{a}}}^{(c)} \triangleq \dfrac{1}{2(n_{\mathrm{a}} + \lambda)}, \\ & \quad i = 1, \dots, n_{\mathrm{a}}, \end{cases}$$

where $\mathrm{col}_i \left[(\cdot)^{1/2} \right]$ is the ith column of the Cholesky square root, $0 < \alpha \leq 1$, $\beta \geq 0$, $\kappa \geq 0$, and $\lambda \triangleq \alpha^2(\kappa + n_{\mathrm{a}}) - n_{\mathrm{a}}$. We set $\alpha = 1$ and $\kappa = 0$ [3] such that $\lambda = 0$ [4] and set $\beta = 2$ [3]. Alternative schemes for choosing sigma points are given in [4].

The UKF *forecast* equations are given by in Appendix A, while the UKF *data-assimilation* equations are given by (2.17)-(2.19).
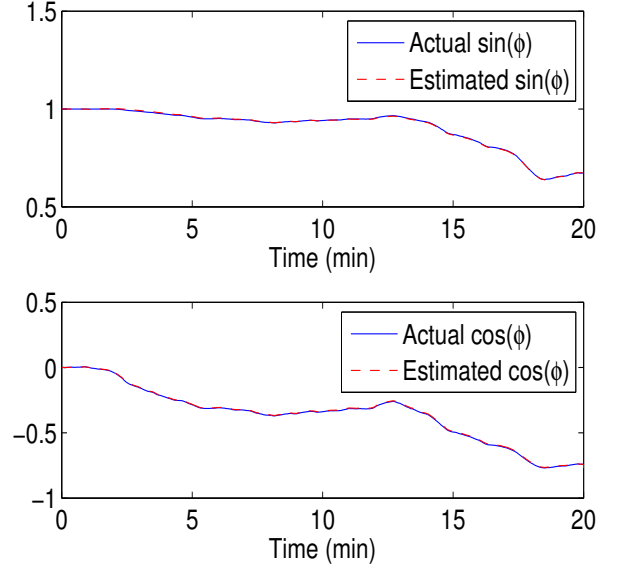

Fig. 5. Actual yaw angle of the buoy and it's estimate. The unscented Kalman filter based on the nonlinear model equations and the rate gyro measurements along with the physics-based fictitious measurement provides an accurate estimate of the actual yaw angle.

Finally, the unscented Kalman filter is applied to estimate the yaw angle of the buoy using a window of time steps, where each time-step is governed by the state equations (5.4) - (5.6). The gyro measurements of angular velocity are used along with the physics-based fictitious measurements. Figure 5 shows the actual values and estimates of the first state ($\sin(\phi)$) and the second state ($\cos(\phi)$). The estimates are seen to match the actual values of the states.

VI. CONCLUSIONS

Magnetic-field fluctuations caused by solar storms can overload and destroy transformers, power grids and sensitive instrumentation on satellites, planes, and ships. To monitor these magnetic-field fluctuations, it was proposed to install magnetometers on floating buoys in the oceans. To obtain meaningful measurements from the magnetometers, it is important to know the orientation of the axes of the magnetometers with respect to the Earth. The goal of this paper was to estimate the orientation of a floating buoy with respect to Earth using gyro measurements of angular velocity of the buoy. Since the angular position states are unobservable from the angular velocity measurements, we constructed an additional physics-based fictitious measurement. In addition, to accommodate the additional fictitious measurement, we used an alternative nonlinear model for the buoy dynamics and a window of time steps in the state-space equations. Furthermore, we used nonlinear filtering techniques to estimate the orientation of the buoy.

REFERENCES

[1] Daum, F. E. Nonlinear filters: Beyond the Kalman filter. *IEEE Aerospace and Electronics Systems Magazine*, **20**(8), 57–69, 2005.

[2] J. D. Glover. The linear estimation of completely unknown systems. *IEEE Trans. on Automatic Contr.*, pages 766–767, December 1969.

[3] Haykin, S. (Ed.) *Kalman Filtering and Neural Networks*. New York – NY, USA: Wiley Publishing, 2001..

[4] Julier, S. J. and Uhlmann, J. K. Unscented filtering and nonlinear estimation. *Proceedings of the IEEE*, 92: 401–422, 2004.

[5] Julier, S. J., Uhlmann, J. K., and Durrant-Whyte, H. F. A new method for the nonlinear transformation of means and covariances in filters and estimators. *IEEE Transactions on Automatic Control*, 45(3): 477–482, 2000.

[6] Kalman, R. E. A new approach to linear filtering and prediction problems. *Transactions of the ASME – Journal of Basic Engineering*, 82: 35–45, 1960.

[7] P. G. Thomasson. Guidance of a Roll-Only Camera for Ground Observation in Wind. *Journal of Guidance, Control, and Dynamics*, 21(1):39–44, 1998.

[8] van der Merwe, R., Wan, E. A., and Julier, S. J. Sigma-point Kalman filters for nonlinear estimation and sensor-fusion – applications to integrated navigation. *Proceedings of the AIAA Guidance, Navigation & Control Conference*. Providence – RI, USA, 2004.

[9] D. H. Hathaway. The solar wind. Solar Physics - Science Directorate, http://science.msfc.nasa.gov/ssl/pad/solar/sun_wind.htm.

[10] S. F. Odenwald. *The 23rd Cycle*. Columbia University Press, February 2001.

[11] I. Sandahl. Does space weather really matter on the ground? In Ling-Hsiao Lyu, editor, *Space Weather Study Using Multipoint Techniques*, volume 12 of *Proceedings of COSPAR*, pages 349–357. September 2000.

VII. Appendix A: UKF Forecast Equations

The UKF *forecast* equations are given by

$$\mathcal{X}_{k-1} = \left[\hat{x}_{k-1}^{\mathrm{a}} \quad \hat{x}_{k-1}^{\mathrm{a}} 1_{1 \times n_{\mathrm{a}}} + \sqrt{(n_{\mathrm{a}} + \lambda)} \left(P_{k-1}^{xx\mathrm{a}}\right)^{1/2} \quad \hat{x}_{k-1}^{\mathrm{a}} 1_{1 \times n_{\mathrm{a}}} - \sqrt{(n_{\mathrm{a}} + \lambda)} \left(P_{k-1}^{xx\mathrm{a}}\right)^{1/2} \right], \tag{7.1}$$

$$\mathrm{col}_i(\mathcal{X}_{k|k-1}^x) = f_{k-1}(\mathrm{col}_i(\mathcal{X}_{k-1}^x), \ u_{k-1}, \ \mathrm{col}_i(\mathcal{X}_{k-1}^w)), \quad i = 0, \ldots, 2n_{\mathrm{a}}, \tag{7.2}$$

$$\hat{x}_{k|k-1} = \sum_{i=0}^{2n_{\mathrm{a}}} \gamma_i^{(m)} \mathrm{col}_i(\mathcal{X}_{k|k-1}^x), \tag{7.3}$$

$$P_{k|k-1}^{xx} = \sum_{i=0}^{2n_{\mathrm{a}}} \gamma_i^{(c)} [\mathrm{col}_i(\mathcal{X}_{k|k-1}^x) - \hat{x}_{k|k-1}][\mathrm{col}_i(\mathcal{X}_{k|k-1}^x) - \hat{x}_{k|k-1}]^{\mathrm{T}}, \tag{7.4}$$

$$\mathrm{col}_i(\mathcal{Y}_{k|k-1}) = h_k(\mathrm{col}_i(\mathcal{X}_{k|k-1}^x)), \quad i = 0, \ldots, 2n_{\mathrm{a}}, \tag{7.5}$$

$$\hat{y}_{k|k-1} = \sum_{i=0}^{2n_{\mathrm{a}}} \gamma_i^{(m)} \mathrm{col}_i(\mathcal{Y}_{k|k-1}), \tag{7.6}$$

$$P_{k|k-1}^{yy} = \sum_{i=0}^{2n_{\mathrm{a}}} \gamma_i^{(c)} [\mathrm{col}_i(\mathcal{Y}_{k|k-1}) - \hat{y}_{k|k-1}][\mathrm{col}_i(\mathcal{Y}_{k|k-1}) - \hat{y}_{k|k-1}]^{\mathrm{T}} + R_k, \tag{7.7}$$

$$P_{k|k-1}^{xy} = \sum_{i=0}^{2n_{\mathrm{a}}} \gamma_i^{(c)} [\mathrm{col}_i(\mathcal{X}_{k|k-1}^x) - \hat{x}_{k|k-1}][\mathrm{col}_i(\mathcal{Y}_{k|k-1}) - \hat{y}_{k|k-1}]^{\mathrm{T}}, \tag{7.8}$$

where $\begin{bmatrix} \mathcal{X}_{k-1}^x \\ \mathcal{X}_{k-1}^w \end{bmatrix} \triangleq \mathcal{X}_{k-1}$, $\mathcal{X}_{k-1}^x \in \mathbb{R}^{n \times (2n_{\mathrm{a}}+1)}$, and $\mathcal{X}_{k-1}^w \in \mathbb{R}^{q \times (2n_{\mathrm{a}}+1)}$.